JOURNAL OF MATERIALS SCIENCE 19 (1984) 202–212

Composite materials made from a porous 2D-carbon–carbon preform densified with boron nitride by chemical vapour infiltration

H. HANNACHE, J. M. QUENISSET, R. NASLAIN
Laboratoire de Chimie du Solide du CNRS, Université de Bordeaux-I 351, Cours de la Libération, 33405 Talence-cédex, France

L. HERAUD
Société Européene de Propulsion, B.P. 37, 33165 Saint Médard-en-Jalles, France

---

2D-C–C/BN composites (with a BN volume fraction (V_{BN}) up to 0.60) have been obtained by chemical vapour infiltration of hexagonal-BN from a BF_3–NH_3 mixture, within the pores of a 2D-C–C preform made of a stacking of carbon fabric layers which has been weakly consolidated with pyrocarbon. They were tested in compression on samples with the carbon fabric layers directed either parallel or perpendicular to the load axis. In the first case (*p*-direction), the compression behaviour is mainly elastic (at least for high enough V_{BN}). Both $\sigma_{\parallel}^{R}$ and $E_{\parallel}$ increase regularly with rising V_{BN}, as the BN-layer deposited within the pores of the preform (mainly located between adjacent carbon layers) becomes thicker. $\epsilon_{\parallel}^{R}$ is weak and progressively decreases with increasing V_{BN}. In the second case (*o*-direction), the stress–strain curve exhibits both elastic and pseudoplastic domains whose respective extension depends on V_{BN} (or on V_p). The pseudoplastic behaviour is related to an irreversible microstructural damage of the interlayer C/BN filling. $\sigma_{\perp}^{R}$, $\sigma_{\perp}^{E}$ and $E_{\perp}$ increase with increasing V_{BN} (or decreasing V_p) according to parabolic laws. $\epsilon_{\perp}^{R}$ is much higher than $\epsilon_{\parallel}^{R}$. The materials remain anisotropic even at high V_{BN}. Oxidation tests in air (or oxygen/argon mixtures) have shown that 2D-C–C/BN, incompletely densified ($V_p \sim 0.10$) by BN, exhibit a weight loss (oxidation of the carbon skeleton) at low temperatures and a weight increase (oxidation of BN) above 900° C. Oxidation resistance is enhanced by increasing V_{BN} (which results in a V_p decrease) and decreasing oxygen partial pressure. It is predicted that a good oxidation protection of the carbon skeleton requires a full densification by BN ($V_p \sim 0$) and will be effective at medium temperatures. The results of the present study could be easily extended to 2D-BN–BN composites.

---

1. Introduction

Hexagonal boron nitride has a layer crystal structure very similar to that of graphite. Furthermore, it is one of the best electrical insulators at high temperature actually known and it has a good chemical inertia (as an example, its oxidation resistance in air is much higher than that of graphite). Boron nitride is easily prepared, amorphous or well crystallized, from different gas mixtures (such as boron halides and ammonia) or by nitriding boron oxide. Despite these features, its use in composite materials, either as fibres or as matrix, has been the subject of very few studies, as compared to the case of carbon [1–8].

A programme has been underway in our laboratories for the last few years to develop composite materials, for high temperature applications, deriving from well known carbon–carbon products by replacing, partly or totally, the carbon matrix by different refractory materials such as

0022–2461/84 $03.00 + .12

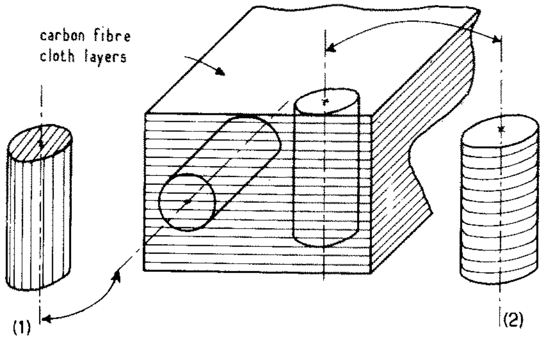

Figure 1 Orientation of the carbon fabric layers in the samples used for the mechanical and oxidation resistance tests.

silicon or titanium carbides [9–13]. It seemed worthwhile to extend the research to hexagonal boron nitride, on the basis of its crystal structure similarity with graphite and of its intrinsic properties at high temperatures.

2. Synthesis of the composite materials

The starting material was a 2D-carbon–carbon preform made of a stack of carbon fabric (woven from medium grade PAN-base fibres for thermal applications) weakly infiltrated with pyrocarbon (resulting from the pyrolysis of methane). The pyrocarbon was used to bind sufficiently the fabric layers together while keeping a large open porosity ($V_{p_0} \sim 0.60$). The samples used for the mechanical and oxidation tests were cut in this preform, either parallel or perpendicular to the fabric layers, as shown in Fig. 1, prior to BN-infiltration.

The available open porosity of the samples was then filled by BN, either partly or almost totally, according to a chemical vapour infiltration process (CVI) which has been described in detail elsewhere [14]. In order to obtain a crystallized BN matrix, a BF_3–NH_3 gas mixture was used, as already suggested by Pierson [5] for the infiltration of BN–fibre felts. The infiltration was performed in a modified LP-CVD apparatus at about 1150° C, 0.026 atm and $\alpha = [NH_3]/[BF_3] = 1.4$. Under such conditions, BN deposition occurs within the pores rather than on the external surface of the samples, leading to a progressive in depth densification of the initial 2D-C–C porous preform. However, the rate of deposition is slow especially when coming close to full densification, as illustrated in Fig. 2. As the infiltration is in progress, BN which is first deposited on the consolidation pyrocarbon, progressively fills all the available open pores, as shown in Fig. 3. It is deposited under the form of the hexagonal graphite-like modification with

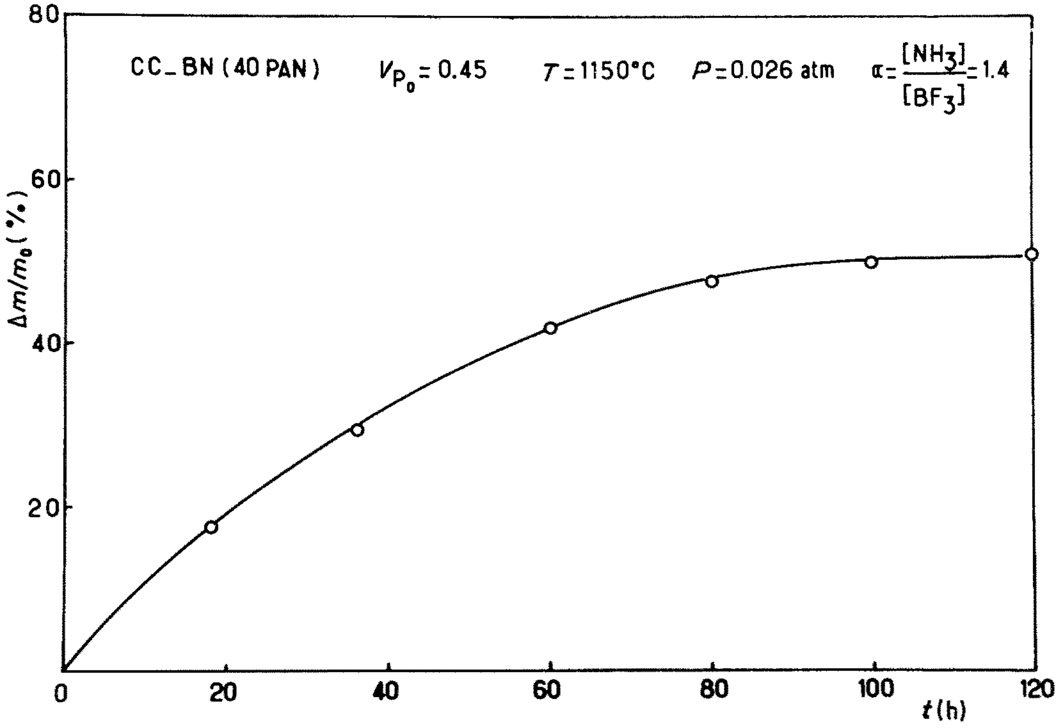

Figure 2 Weight increase against time during the chemical vapour infiltration of hexagonal BN within the pores of a 2D-C–C preform, from a BF_3–NH_3 gas mixture.

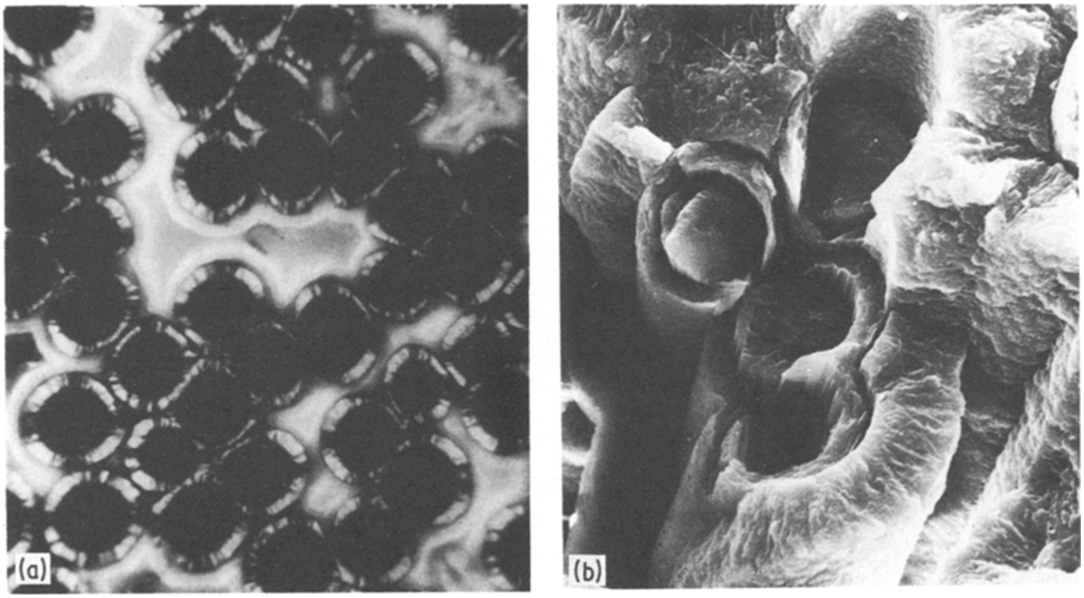

Figure 3 Microstructure of 2D-C–C/BN composites obtained by CVI of BN in the pores of a 2D-C–C preform: (a) polished section observed under polarized light; (b) surface of failure (SEM).

crystal defects similar to those observed for pyrocarbon deposited at the same temperature (Fig. 4). The resulting composites, characterized by a 2D-carbon fibre reinforcement and a C/BN hybrid matrix will be referred to as 2D-C–C/BN.

2D-C–C/BN composites were characterized from a mechanical and chemical point of view, on a series of samples prepared from the same 2D-C–C preform (with a fixed initial open porosity V_{p_0} of the order of 0.50–0.60) and containing increasing volume fractions of BN ($0 < V_{\mathrm{BN}} < V_{\mathrm{p}_0}$) and therefore having decreasing residual porosities V_p ($V_{\mathrm{p}_0} > V_\mathrm{p} > 0$) since $V_{\mathrm{BN}} + V_\mathrm{p} = V_{\mathrm{p}_0} =$ constant.

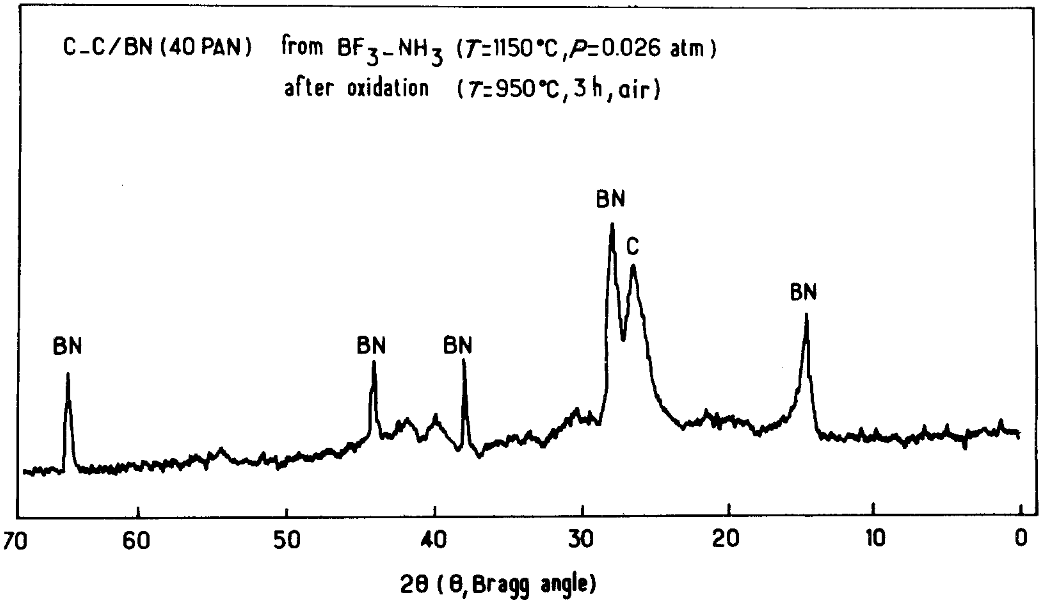

Figure 4 Debye–Scherrer pattern of BN deposited from a BF_3–NH_3 mixture within the pores of a 2D-C–C preform and partly separated from the carbon skeleton by oxidation in air at 950° C.

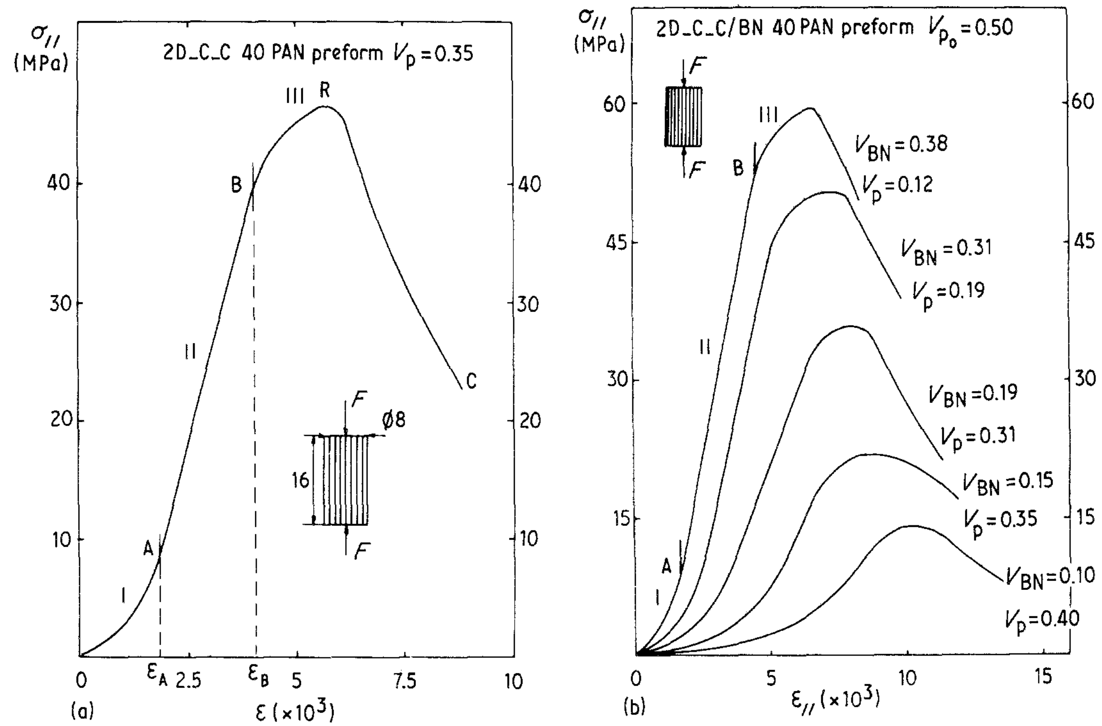

Figure 5 Compression behaviour of 2D-C–C/BN composites loaded parallel to the carbon fabric layers: (a) stress–strain curve for the initial 2D-C–C preform, (b) stress–strain curves for 2D-C–C/BN with various V_{BN} values.

3. Mechanical characterization in compression

The materials were characterized in compression on cylindrical samples ($h = 16$ mm, $\phi = 8$ mm), the carbon fabric layers being either parallel or perpendicular to the cylinder axis. The samples were tested, in the so-prepared conditions (no further machining was performed after the BN-CVI step) with a deflection rate of 0.1 mm min^{-1}.

3.1. Compression tests parallel to the carbon fabric layers

The main features of the stress–strain curves of 2D-C–C/BN composites, loaded parallel to the carbon fabric layers, are shown in Fig. 5. The strain axis can be schematically divided into three domains.

3.1.1. Domain I

For $0 < \epsilon_{\|} < \epsilon_{\|}^{A}$ a nonlinear stress–strain relationship is observed corresponding to a progressive (but not permanent) rigidification (Fig. 5a). The higher V_{BN} the more pronounced this rigidification effect but the lower is $\epsilon_{\|}^{A}$ (Fig. 5b). During this period the numerous elementary beams constituting the material find their fulcrums within the still porous layer microstructure.

3.1.2. Domain II

For $\epsilon_{\|}^{A} < \epsilon_{\|} < \epsilon_{\|}^{B}$ the compression behaviour of the material appears to be elastic. The Young's modulus $E_{\|}$ is the slope of the stress–strain curve.

The rigidity of 2D-C–C preforms only slightly infiltrated with BN (e.g. $V_{BN} = 0.10$ or 0.15) is quite weak, this feature being related to the poor compression rigidity of the initial preform and to the low BN elastic modulus. Increasing V_{BN} (and therefore decreasing V_p) raises the cross-section as well as the bending stiffness of each elementary beam of the microstructure and leads to an increase in the compression bulk modulus $E_{\|}$.

In opposition with other infiltrated materials such as TiC, the relationships between $E_{\|}$ (or $\sigma_{\|}^{R}$) and V_{BN}, as experimentally established, do not exhibit any significant break, as soon as V_{BN} is increased (Fig. 6) [12, 13]. This feature could be explained by the much lower value of E_{BN} as compared to E_{TiC}. For low V_{BN} no cracks occur in the BN deposit (that would lead to the weak stiffness of the initial preform) when the 2D-C–C/BN composite is strained in domain I.

3.1.3. Domain III

For $\epsilon_{\|} > \epsilon_{\|}^{B}$ the material starts to become irre-

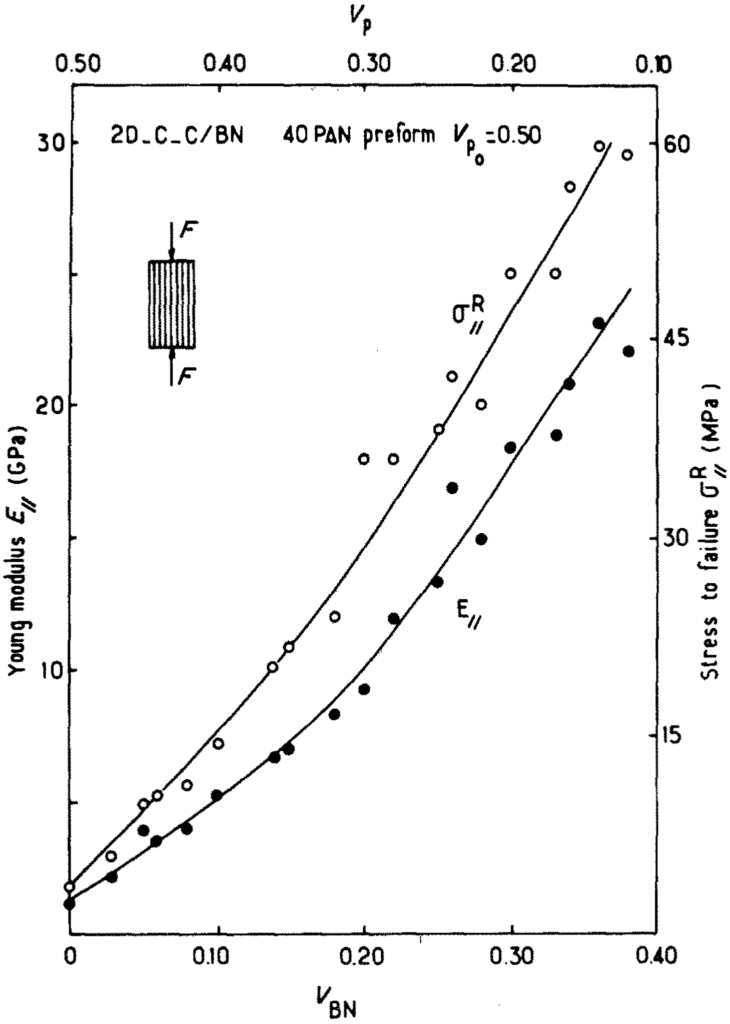

Figure 6 Variations of the strength to failure $\sigma_{\|}^R$ and Young's modulus $E_{\|}$ against V_{BN} for 2D-C–C/BN composites loaded parallel to the carbon fabric layers.

versibly damaged by numerous cracks within the BN deposit, not particularly along the elementary beams of the microstructure (as occurred for highly densified 2D-C–C/TiC composites), but mostly between the fabric layers whose free length increases progressively leading to a rising buckling. When the free length of the fabric layers is long enough an instability takes place resulting in a failure by delamination. It appears thus that 2D-C–C/BN composites behave as the related 2D-C–C materials due to the rather low value of the BN modulus.

Otherwise, when V_{BN} is increased, the cross-section of each elementary beam of the microstructure becomes larger. Thus, the rupture strain of the beams becomes smaller and smaller, with the result that the load leading to the failure of the material is larger. In other words increasing V_{BN} increases $\sigma_{\|}^R$ and simultaneously decreases $\epsilon_{\|}^R$ (Fig. 5b).

3.2. Compression tests perpendicular to the carbon fabric layers

The stress–strain curves corresponding to 2D-C–C/BN composites with increasing V_{BN} values, loaded in compression perpendicular to the carbon fabric layers, are shown in Fig. 7.

It appears from Figs. 5 and 7 that the main features of the stress–strain curves of the 2D-C–C/BN composites are very different according to the direction along which the load is applied. When the load is applied perpendicularly to the fabric layers, the strain axis can be divided into four domains:

(a) for low $\epsilon_{\perp}$ values (domain I), a nonlinear stress–strain relationship is observed, immediately followed by a domain of "elastic behaviour" (domain II) which corresponds to a Young's modulus $E_{\perp}$. It appears that the extension of this domain of elastic behaviour increases as the pores of the initial 2D-C–C preform are progressively

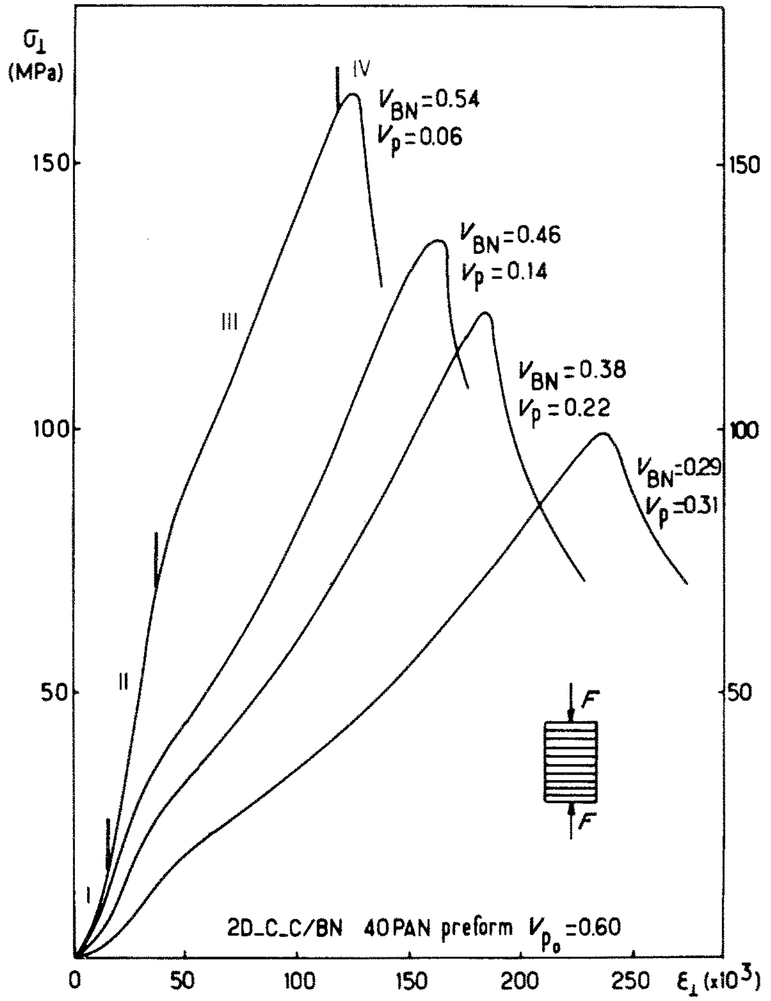

Figure 7 Compression behaviour of 2D-C–C/BN composites loaded perpendicular to the carbon fabric layers.

filled with BN (or as the residual porosity V_p decreases). It is still rather limited for $V_{BN} = 0.31$ (or $V_p = 0.29$), but it becomes greater for a material almost fully densified ($V_{BN} = 0.54$; $V_p = 0.06$).

(b) for $\epsilon_\perp > \epsilon_\perp^E$, a wide domain of "nonlinear" stress–strain relationship is found (domain III). This domain of "pseudo plasticity" may correspond to a microstructural modification of the composite, the applied load progressively breaking the pyrocarbon/hexagonal BN hybrid interlayer bridges and thus bringing closer together the carbon fabric layers. Although this phenomenon must be regarded as an "irreversible microstructural damage", it results in an important strength increase. Within this domain, the stress–strain relationship is of exponential type. The extension of this domain decreases with increasing V_{BN}, as that of domain II increases. Finally, failure occurs for $\epsilon_\perp^R$ in domain IV.

These features are very similar to those reported by Rossignol *et al.* [13], for the related 2D-C–C/TiC composites. In the same manner it has been found here that the strain to failure $\epsilon_\perp^R$ is much higher (of the order of 100 to 300 x 10^{-3}) than that measured in the *p*-direction, i.e. $\epsilon_\parallel^R$ (of the order of 5 x 10^{-3}), a feature which is related to microstructural considerations.

The variations of $E_\perp$, $\sigma_\perp^R$ and $\sigma_\perp^E$, as a function of V_{BN} (or of V_p), are shown in Fig. 8. The first amounts of BN deposited within the pores of the 2D-C–C preforms do not yield a significant increase in $E_\perp$, $\sigma_\perp^R$ or $\sigma_\perp^E$ since the mechanical characteristics of pyrolytic BN are rather weak. When the infiltrated BN layer becomes thick enough, a significant increase in both strength and modulus is observed. Although the data reported in Fig. 8 are characterized by some scattering, it seems that they could be fitted to parabolic laws.

Finally, 2D-C–C/BN composites remain aniso-

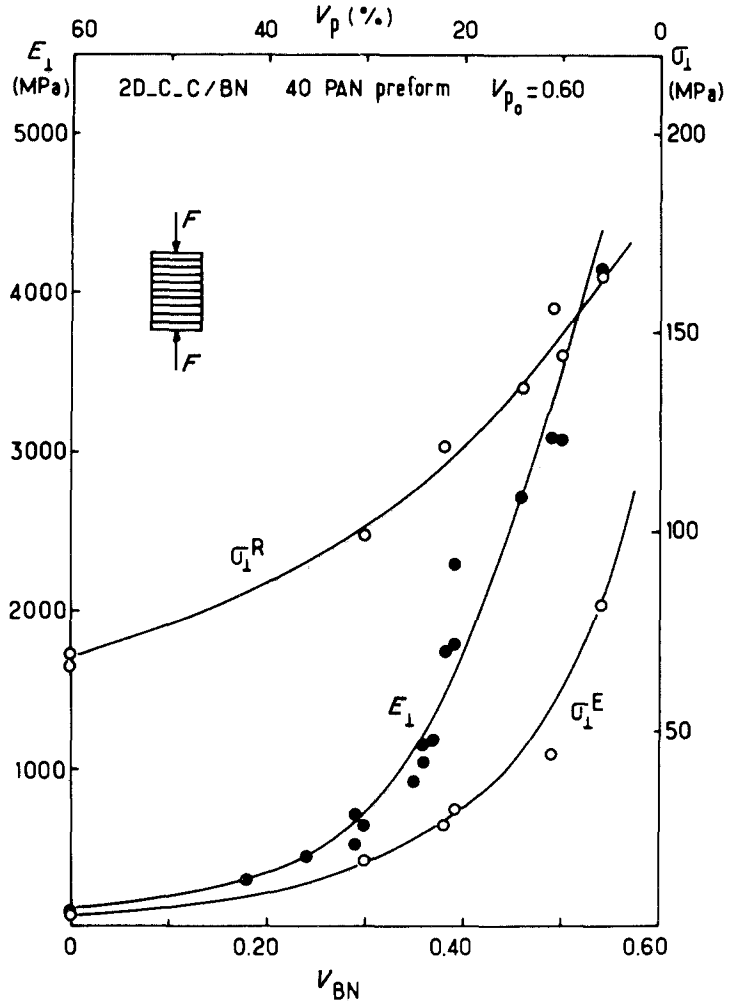

Figure 8 Variations of $\sigma_\perp^R$, or $\sigma_\perp^E$ and $E_\perp$ against V_{BN} for 2D-C–C/BN composites loaded perpendicular to the carbon fabric layers.

tropic materials (with higher mechanical characteristics in the o-direction), even for high V_{BN} values, whereas 2D-C–C/TiC composites were reported to be regarded as almost isotropic when the volume fraction of TiC becomes high enough [12, 13]. This feature can be explained by the fact that the stiffness of pyrolytic BN is not high enough to eliminate the initial preform anisotropy.

4. Oxidation resistance

Since conventional 2D-C–C composites are known to have a poor oxidation resistance even at medium or low temperatures (with a weight loss), oxidation tests were performed in air, for the sake of comparison, on the related 2D-C–C/BN composites. The experiments were run on samples ($\phi = 8$ mm; $h = 8$ mm) whose carbon fabric layers were perpendicular to the cylinder axis, as a function of temperature, time, partial oxygen pressure and V_{BN} (or V_p). The sample was set on a platinum holder and temperature was measured by a Pt-Pt/10Rh thermocouple. The weight variation of the sample was continuously recorded against time.

The influence of temperature on the weight variations of the samples is shown in Fig. 9 (each sample was heated from room temperature to the test temperature under argon and then kept for four hours in air at the test temperature).

At low temperatures, i.e. $\theta < 900°$ C, a weight loss is observed. This is low, but already significant at 600° C and progressively increases as temperature is raised up to 900° C. This weight loss may be interpreted as being mainly the result of the oxidation of the carbon fabric layers (i.e. carbon fibres and/or pyrocarbon of consolidation), with an evolution of carbon oxides, the oxidation of BN being known as very low under such conditions. Thus the occurrence of this weight loss shows that the carbon preform is not totally protected by the BN deposit as it could be predicted

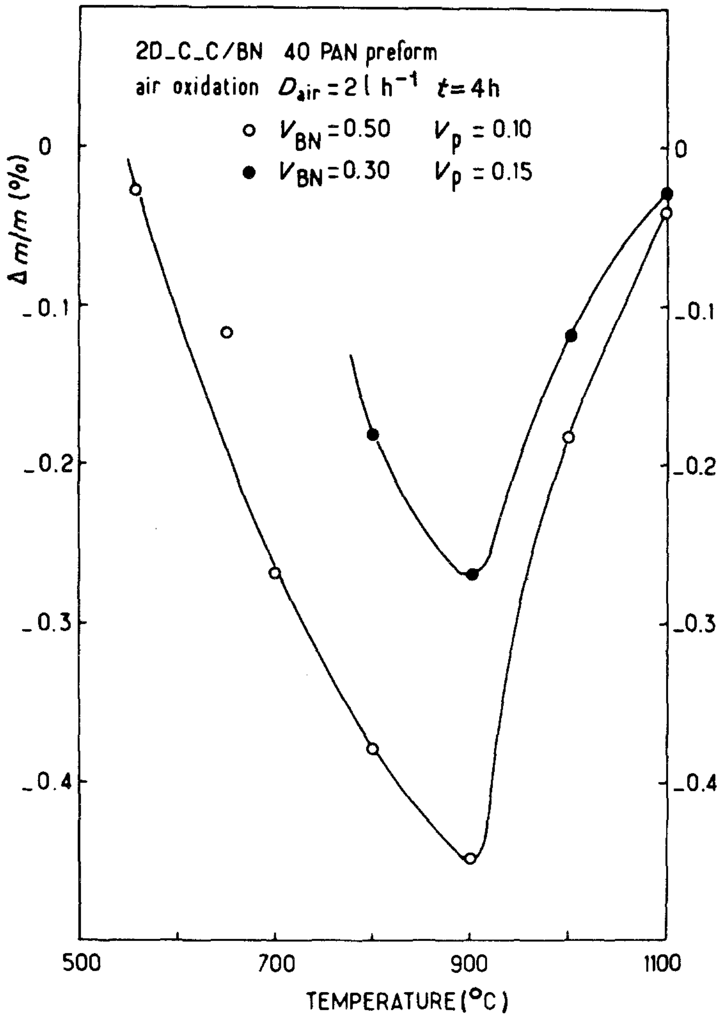

Figure 9 Weight variations of 2D-C–C/BN composites after a 4 h oxidation test in air at increasing temperatures.

from the fact that the material tested still contained some residual porosity (10 to 15%).

At high temperatures, i.e. $\theta > 900°$ C, a weight increase occurs. This is attributed to the oxidation of the BN deposit which results in the formation of a glassy B_2O_3 film at the surface of the sample, according to the overall equation:

$$2BN_{(s)} + \tfrac{3}{2}O_{2(g)} \longrightarrow B_2O_{3(l)} + N_{2(g)}. \quad (1)$$

This B_2O_3 film can, at least partly, slow down the diffusion rate of oxygen through the BN-deposit defects (microcracks, pores only partly filled) towards the 2D-C–C skeleton, resulting in a protection against oxidation (at least in the 900–1100° C temperature domain considered here). It appears from Fig. 9 that the weight increase variation against temperature slightly slows down as temperature reaches 1000–1100° C. This feature could be the result of a slight vaporization of the B_2O_3 liquid film.

The influence of the BN volume fraction (and of the related residual porosity) on the oxidation behaviour of the 2D-C–C/BN composites at 900° C is shown in Fig. 10. At low V_{BN} values (i.e. for preforms weakly densified with BN and still characterized by a high residual porosity), the 2D-C–C preform, which is only poorly protected by the small amount of BN deposited, is strongly oxidized. The material undergoes an important weight loss. The lower V_{BN} (and thus the higher V_p) the larger the weight loss for a given oxidation time. As the oxidation progresses, the oxidation rate tends to become almost constant. On the contrary, at high V_{BN} values (i.e. for preforms highly densified and characterized by a low residual porosity) almost no weight variation is observed. This feature could receive two different interpretations: (a) for materials which are almost fully densified, the BN deposit does act as an efficient protection of the 2D-C–C skeleton, or

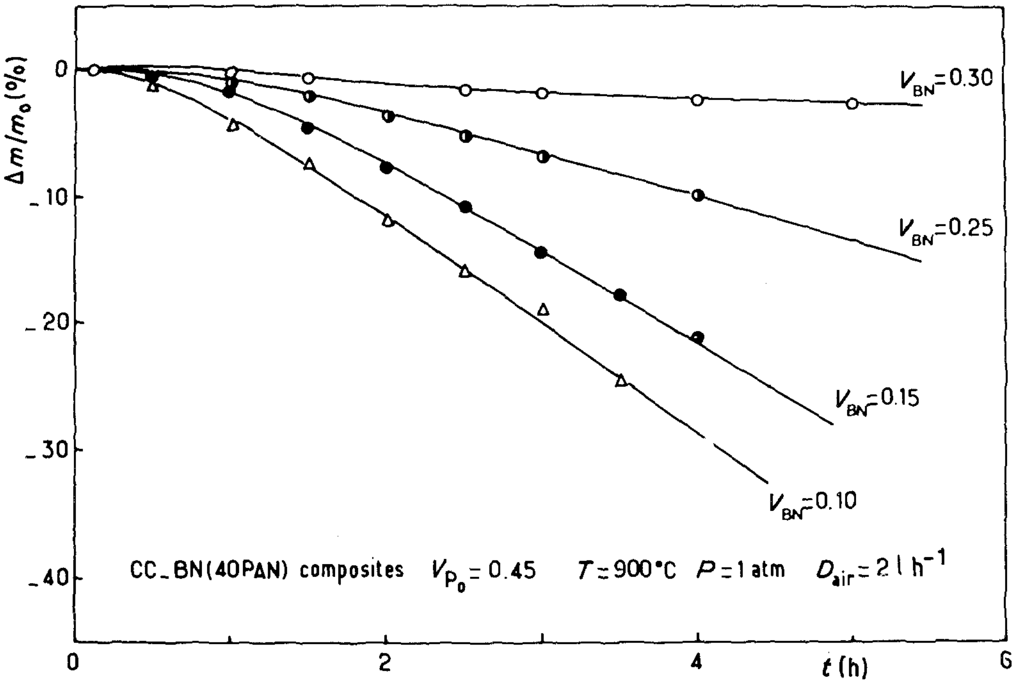

Figure 10 Influence of V_{BN} (and of V_p) on the oxidation kinetics of 2D-C–C/BN composites in air and at 900° C.

(b) the oxidation of BN (corresponding to a weight increase) just compensates that of carbon (corresponding to a weight loss).

The influence of the oxygen partial pressure in the gas mixture (oxygen/argon) on the oxidation behaviour of 2D-C–C/BN composites at 1100° C is illustrated in Fig. 11. At very low oxygen concentrations (e.g. 2 vol%) almost no weight loss is observed despite the high value (1100° C) of the test temperature and the still high residual

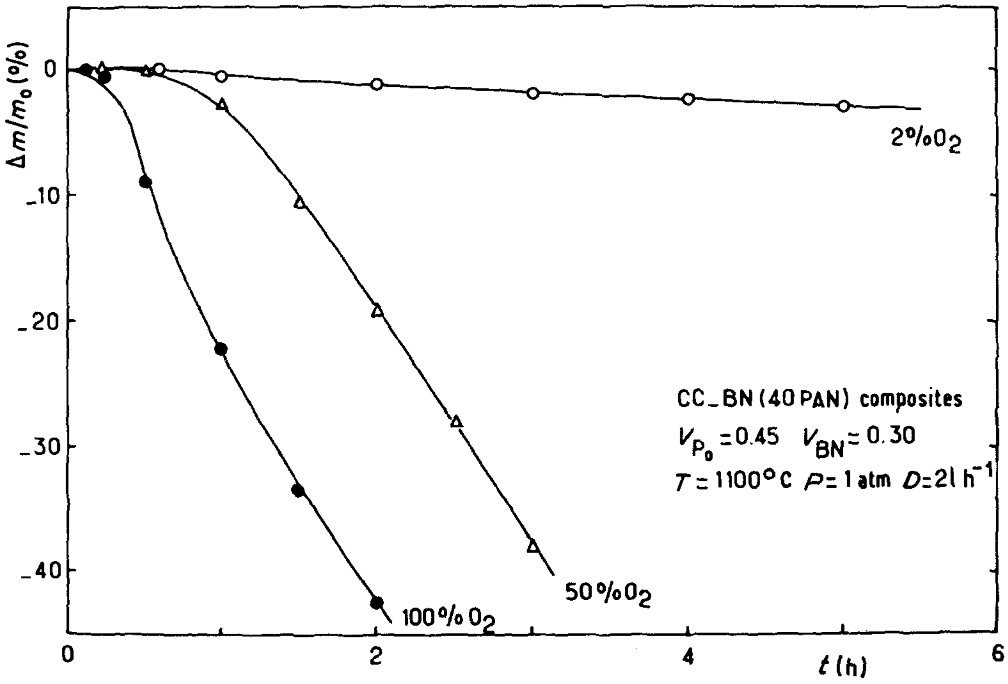

Figure 11 Influence of the partial oxygen pressure on the oxidation kinetics of 2D-C–C/BN composites at 1100° C in an argon–oxygen gas mixture.

porosity of the material ($V_{BN} = 0.30$; $V_p = 0.15$). On the contrary, at high oxygen concentration (e.g. 50 vol % or pure oxygen), the weight loss is very large, the protection effect due to BN and the liquid B_2O_3 film being not extended enough (the residual porosity is too high) to reduce markedly the oxygen diffusion towards the 2D-C–C skeleton. Under such conditions some weight loss due to B_2O_3 vaporization is also possible, as already stated above.

The results of the present study corroborate those reported by Christin and co-workers [9–11], for the related 2D-C–C/SiC composites, according to which a 2D-C–C preform is well protected against an oxidizing agent (such as air) only when it is fully densified with SiC ($V_p \sim 0$). In the same manner Rossignol *et al.* [13] have drawn a similar conclusion in the case of the 2D-C–C/TiC composites, with the difference that the oxidation protection due to TiC is much less efficient than that due to SiC especially at high temperatures.

Thus, it can be predicted that the oxidation resistance of 2D-C–C/BN composites, obtained by BN-CVI within the pores of a 2D-C–C preform, could still be significantly increased, with respect to the results reported here, for materials fully densified ($V_p \sim 0$) and properly optimized. However, it remains that the oxidation resistance of 2D-C–C/BN composites (or even of BN–BN composites that could be made from BN fibre fabric) will be lower than that of the related 2D-C–C/SiC (or 2D-SiC–SiC) composites due to the higher thermal stability and lower volatility of SiO_2 with respect to B_2O_3.

Finally, the results of the present study are in good agreement with those of oxidation tests performed by Economy and Lin [15] on BN fibres, showing that BN fibres begin to be significantly oxidized above about 900° C.

5. Conclusions

Chemical vapour infiltration utilizing a BF_3–NH_3 gas mixture appears to be an efficient way to introduce hexagonal boron nitride in the pores of a fibrous preform, even when the available open porosity is rather low (pores of small diameter). However, it has to be performed at low temperature and total pressure. Under such conditions, the deposition rate is necessarily low but of the same order as those previously reported for pyrocarbon or silicon carbide.

When a 2D-C–C preform is used as starting material, the process leads to 2D-C–C/BN composites having a carbon fibre skeleton and a C/BN hybrid matrix. Their mechanical properties in compression have common features either with those of 2D-C–C composites or with those of the related 2D-C–C/SiC or 2D-C–C/TiC composites previously investigated. However, the mechanical strength and modulus of the 2D-C–C/BN composites are lower than those of the latter ones as BN is less stiff than both SiC and TiC. They could be better compared to those of the former materials on the basis of the structural similarity between hexagonal BN and graphite, and of the low stiffness of pyrolytic BN. Finally 2D-C–C/BN composites remain anisotropic materials even for high V_{BN} values.

2D-C–C/BN composites must have a good oxidation resistance at medium temperatures (up to about 1000° C) provided they have been fully densified ($V_p \sim 0$). Under such conditions, the 2D-C–C preform will be well protected against oxidation by both BN matrix and B_2O_3 film resulting from the surface oxidation of BN. However, any defects in the BN deposit will permit an in depth diffusion of oxygen and an oxidation of the carbon preform. This drawback could be overcome by replacing the carbon fibres by BN fibres, but the latter have much weaker mechanical performances and are not presently available in large quantities.

Acknowledgements

The authors wish to thank Dr L. Rabardel from CNRS-LCS, Talence as well as Dr J. P. Coutures from CNRS-LUR, Odeillo, for their assistance in the oxidation tests. This work was supported by the French Ministry of Research and Industry under a joined contract SEP/LCS.

References

1. J. ECONOMY and R. V. ANDERSON, *J. Polym. Sci. Part C* 19 (1967) 283.
2. *Idem*, US Patent 3429 722, Feb. 25 (1969).
3. *Idem*, US Patent 3620 780, Nov. 16 (1971).
4. J. ECONOMY and R. Y. LIN, US Patent 3668 059, June 6 (1972).
5. H. O. PIERSON, *J. Compos. Mater.* 9 (1975) 228.
6. R. Y. LIN, J. ECONOMY and H. D. BATHA, *Ceram. Bull* 55/9 (1976) 781.
7. R. Y. LIN, J. ECONOMY, H. H. MURTY and R. OHNSORG, *Appl. Polym. Symp.* 9 (1976) 175.
8. J. J. GEBHARDT, in "4th International Conference on Chemical Vapor Deposition", Abstract 232 (1973) pp. 581–582.

9. F. CHRISTIN, R. NASLAIN and C. BERNARD, in "7th International Conference on Chemical Vapor Deposition", edited by T. O. Sedwick and H. Lydtin, (The Electrochemical Society, Princeton, 1979) pp. 499–514.
10. R. NASLAIN, P. HAGENMULLER, F. CHRISTIN, L. HÉRAUD and J. J. CHOURY, ICCM-3 "Advances in Composite Materials", Vol. 2, edited by A. R. Bunsell, C. Bathias, A. Martrenchar, D. Menke, and G. Verchery (Pergamon Press, New York, 1980) pp. 1084–97.
11. L. HÉRAUD, F. CHRISTIN, R. NASLAIN and P. HAGENMULLER, in "7th International Conference on Chemical Vapor Deposition", edited by J. M. Blocher *et al.* (The Electrochemical Society, Pennington, 1981) pp. 782–89.
12. R. NASLAIN, J. Y. ROSSIGNOL, P. HAGENMULLER, F. CHRISTIN, L. HÉRAUD and J. J. CHOURY, *Rev. Chim. Minér.* 18 (1981) 544.
13. J. Y. ROSSIGNOL, R. NASLAIN, P. HAGENMULLER and L. HÉRAUD, ICCM-4, Tokyo, October 1982, Vol. 2, edited by T. Hayashi, K. Kawata and S. Umekatawa (JSCM Tokyo, 1982) pp. 1227–39.
14. H. HANNACHE, R. NASLAIN and C. BERNARD, *J. Less-common Met.* in press.
15. J. ECONOMY and R. LIN, in "Boron and Refractory Borides", edited by V. I. Matkovich (Springer-Verlag, Heidelberg, New York, 1977) pp. 552–64.

Received 7 April
and accepted 13 May 1983